KWS-2, the high intensity / wide *Q*-range small-angle neutron diffractometer for soft-matter and biology at FRM II

2012 J. Phys.: Conf. Ser. 351 012026

(http://iopscience.iop.org/1742-6596/351/1/012026)

KWS-2, the high intensity / wide *Q*-range small-angle neutron diffractometer for soft-matter and biology at FRM II

A Radulescu[1], V Pipich, H Frielinghaus and M-S Appavou

Forschungszentrum Jülich GmbH, Jülich Centre for Neutron Science (JCNS), Outstation at FRM II, 85747 Garching, Germany

E-mail: a.radulescu@fz-juelich.de

Abstract. The KWS-2 small-angle neutron diffractometer operated by JCNS at FRM II is upgraded and optimized towards high intensity and wide *Q*-range studies of mesoscopic structures and structural changes due to rapid kinetics and becomes a dedicated SANS instrument to soft-matter and biology. The high intensity permits fast measurement of small or weak scattering samples and time resolved structural studies with a time resolution up to 100ms. The possibility to cover up to four decades in *Q* will soon enable structural investigation over a wide length scale, between several Å and 1μm. The characteristics and performance of the instrument in the conventional pinhole mode is detailed presented and the new upgrades currently in progress and aiming for boosting the instrument performance towards higher intensity and wider *Q*-range are reported.

1. Introduction

After the shut-down of the FRJ-2 "DIDO" research reactor in Jülich, the small-angle neutron diffractometers KWS-1 and KWS-2 have been rebuilt by the Jülich Centre for Neutron Science (JCNS) at the neutron source Heinz Maier-Leibnitz (FRM II reactor) in Garching [1]. Both instruments are 42m long and based on the same concept: by the pinhole geometry the exploration of a wide momentum transfers *Q*, between $7x10^{-4}$ and $0.5Å^{-1}$, is possible by the variation of the sample-to-detector distance between 1m and 20m and of the wavelength between 4.5Å and 20Å. At FRM II the combination of the high flux supplied by the cold neutron source (CNS) and the newly designed neutron guide system [2] supported the major upgrade of KWS-2 towards particular scientific topics: with a new "fast" detection electronics accepting high count rates up to 0.6 MHz, a new collimation system allowing for larger experimental flexibility and the routine use of large beam-sizes, KWS-2 became a dedicated SANS diffractometer to high-intensity / wide *Q*-range investigation of mesoscopic structures and structural changed due to rapid kinetics in soft-matter, chemistry and biology.

In the middle of 2010 the instrument entered a second phase of major upgrade aiming for boosting the instrument performance towards higher intensities and wider *Q*-range by means of focusing elements – the MgF_2 lenses [3-5]. The neutron lenses are planned for the high intensity mode (up to 15 times gain in intensity compared to the conventional pinhole mode by increasing the sample area while holding the resolution) and the high resolution mode (exploration of low *Q* range up to $1x10^{-4}$

[1] To whom any correspondence should be addressed.

Å^{-1}) when they will be used in the combination with a double-disk chopper with variable opening and a high resolution position-sensitive detector.

In this paper we will present the design and characteristics of the KWS-2 SANS diffractometer in the standard pinhole mode including some data for demonstrating its performance.

2. Instrument components and characteristics

The 42m long instrument KWS-2 occupies an end-of-guide beam position (50x50mm^2 cross section) on the newly built NL3-ao vertically "S-shaped" neutron guide [2,6] in the cold-neutron-guides West-Hall of FRM II. A conceptual design of the KWS-2 instrument is shown in figure 1 while the key components and working procedure for the pinhole standard mode are discussed in turn below. A detailed description and characterization of the new components that are currently in construction (the double-disc chopper with variable opening, the neutron lenses and the high-resolution detector) makes the subject of a forthcoming publication.

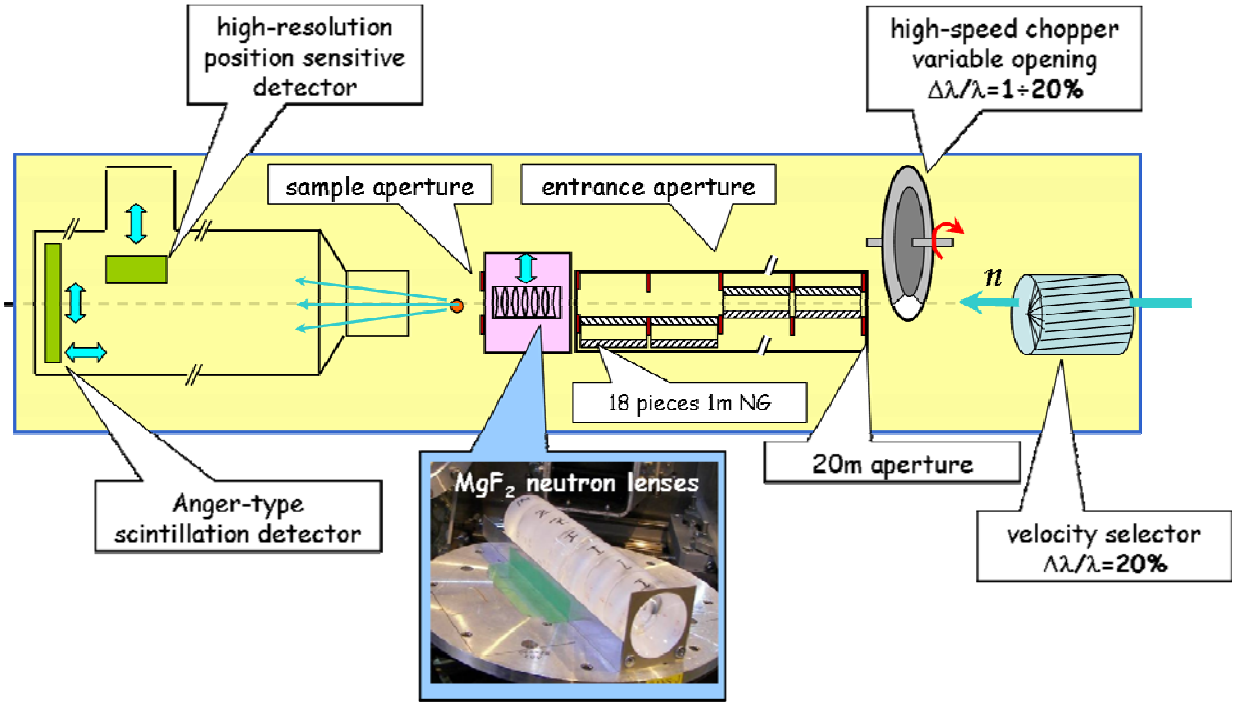

Figure 1. Schematic diagram of the KWS-2 SANS instrument.

2.1. Wavelength selection and collimation system

The incident beam from the neutron guide is monochromatized by a mechanical slit selector (ASTRIUM GmbH) with a wavelength resolution $\Delta\lambda/\lambda=0.20$ in a wavelength range of $\lambda = 4.5 \div 20$Å. The monochromated beam is collimated by a system of moveable guides and fixed position apertures. The 18 neutron guide elements, each 1m long with 50x50mm^2 cross-section and m=1.4 non-magnetic coating, allow for the variation of the effective source-to-sample distance from 2m to 20m in 1m increments to vary the beam divergence and flux on the sample. Each guide is followed by a squared source-defining aperture (entrance aperture). The apertures placed at 2, 4, 8, 14 and 20m in front of the sample and the sample aperture have variable opening, between 1x1mm^2 and 50x50mm^2, allowing for either symmetric or slit-like beam geometry; the other apertures have a 50x50mm^2 fixed opening. All apertures are equipped with ^{10}B enriched ceramic blades with sharp edges and large BC_4 masks. The variable opening apertures are equipped with additional elements that increase their performance (transducers, special driving systems, special positioning and alignment systems). Thus, collimation of

the incident beam is defined by the entrance aperture (typically 50x50mm^2 for standard pinhole mode) and the sample aperture (typically 10x10mm^2); this is the pinhole standard working mode.

2.2. The sample area

The KWS-2 SANS instrument has a sample area that allows for the accommodation of large sample environments such us cryostats, furnaces, rheometers, shear cells, stretching devices, pressure cells, humidity cells, etc. A sample stage that allows for the xyzθ positioning of sample holders and can support heavy sample environments is typically used. In this case, an evacuated tube with variable length, the so-called "collimation nose", enables the positioning of the sample aperture very close to the sample or the entrance window of the sample environment, diminishing the air flight path of neutrons. For measurements at room temperature or within a typical temperature range for soft-matter and biology topics (-20°C÷150°C) a multi-position / multi-level thermostated sample holder with dry-air flow is routinely used. For special cases, an evacuated sample chamber allowing for the use of a multi-position thermostated sample holder with sealed sample cells can be used. The sample area is massively shielded by 1.5cm thick inner layer of borated plastic and 5cm thick outer layer of lead. The access of users at the sample position is allowed through a motorized door commanded by the instrument controlling computer and coordinated with the status of the instrument shutters.

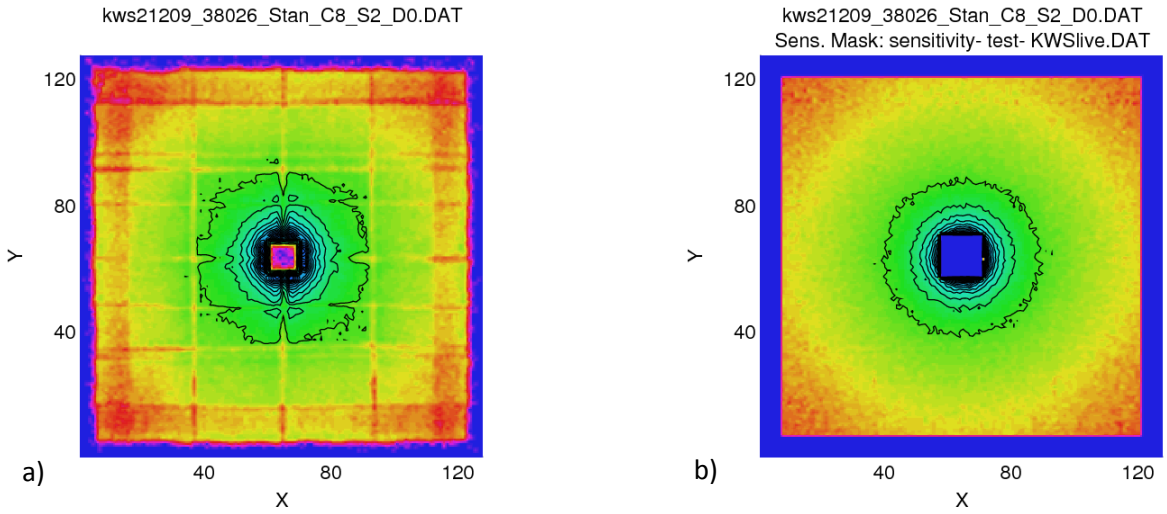

Figure 2. Typical scattering pattern collected with the scintillation detector of KWS-2 as raw data (a) and corrected data for detector sensitivity (b).

2.3. Main detector

The KWS-2 main detector is based on the Anger principle [7] with an array of 8x8 photomultipliers, a 60x60cm^2 ^{6}Li glass scintillator with an efficiency >95% for λ>4.5Å neutrons [8] and a light disperser glass, which spread the light produced by a neutron event to an array of 3x3 photomultipliers [9]. The readout electronics enables fast signal and data processing (about 0.6μs statistical dead-time) and allows for the acquisition of stable and reliable count rates up to 0.6MHz. Because of the photomultipliers array and the scintillator active area made of 4x4 plates glued together, a grid-like structure corresponding to detector regions with lower sensitivity characterizes the raw scattering patterns (figure 2a). Therefore, corrections that take into account the detector sensitivity measured with an incoherent standard sample (Plexiglas) must be always applied to the raw data (figure 2b).

The determination of the system dead-time was carried out by comparing the detector count rates under uniform neutron illumination to that of a fission chamber. Because the count rate of the fission chamber is linearly related to the true count rate n of the scattered neutrons, the dead time of the detector may be derived from the deviations of the measured count rates n_m from the ideal behavior

(figure 3). The recorded data can be fully corrected for detector dead-time losses for count rates up to 150kHz, when a 10% dead-time effect occurs in the measured rates n_m compared to the true rates n (figure 4). The ^{6}Li scintillator is sensitive for γ-radiation originating directly from the reactor or from activated materials in the surroundings. In order to suppress the γ-background discriminators and filtering algorithms have been implemented that reduce the γ-to-neutron ratio to 10^{-5}. The spatial resolution of the detector determined using an absorbing boron coated diaphragm with holes placed in front of the scintillator is 5.25mm.

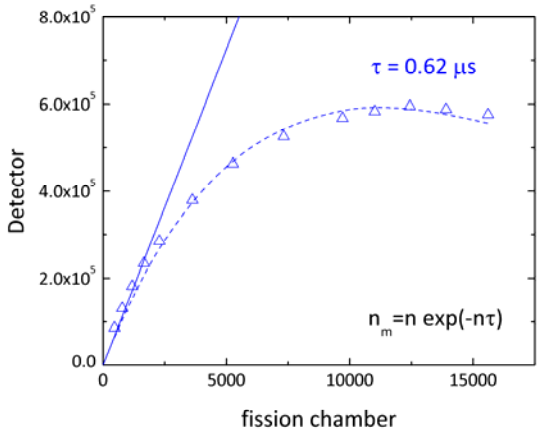

Figure 3. Measurement of the detection electronics dead-time using a "zero dead-time" fission chamber; the fit of the data with the paralysable model (curve) delivered the statistical dead-time; the ideal behavior of the detection electronics is indicated by the straight line.

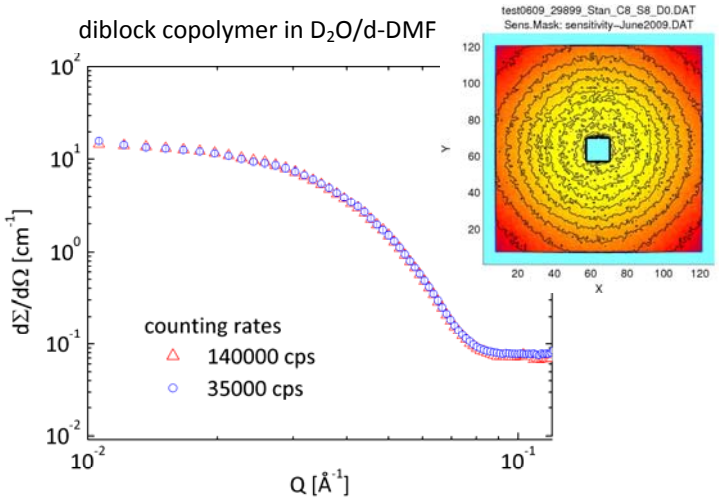

Figure 4. Radially-averaged scattering patterns from a diblock copolymer in solution, measured for different count rates; the data were corrected for the detector sensitivity, scattering from empty cell and instrument background and calibrated on the absolute scale using a Plexiglas secondary standard; the inset show the two-dimensional scattering pattern recorded with a count rate of 140 kHz; the quality of data in both presentations proves the reliability of the dead-time and detector sensitivity corrections applicable up to high count rates.

The main detector is equipped with a system of three mobile rectangular beam-stop masks with sizes of 5x5, 7x7 and 9x9 cm^2, which can be separately brought in beam in order to mask the direct beam and to tune the Q_{min} resolution by matching different beam size and divergence conditions. The detector can be moved between 1m and 20m after the sample and positioned vertically and laterally in beam, in order to catch on the beam-stop the direct beam for different wavelengths.

3. Instrument performance

3.1. Flux at the sample position

The flux at the sample position as a function of the incident wavelength and collimation configuration has been measured by standard gold foil activation method [10]. The results are shown in figure 5.

The magnitude of the neutron flux strongly depends on the amount of liquid deuterium in the cold neutron source (CNS) of FRM II: the full filling of the CNS requires about 15l of it. Detailed flux measurements have been carried out for the partial CNS filling of 10.6l. The highest flux for the shortest collimation length L_c=2m and λ=4.5Å is about 2x10^8 n/s cm^2. Later measurements using the Plexiglas secondary standard performed for a better CNS filling (13l) have shown a considerable increase in the neutron flux at the sample position by a factor of 1.7. Under the optimal conditions of CNS the neutron flux is comparable to that of the SANS instruments at the high-flux reactor of the Institute Laue-Langevin in Grenoble.

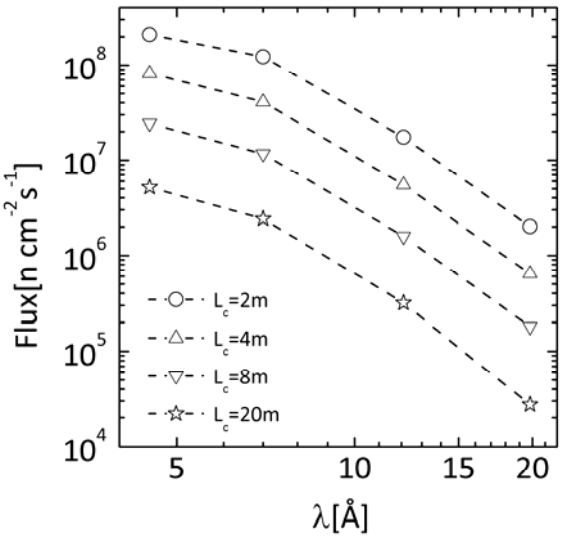

Figure 5. Absolute neutron flux at the sample position as a function of wavelength λ for different collimation lengths L_c, typical opening of the entrance and sample apertures and 10.6l CNS filling.

3.2. Available Q-range

The momentum transfer *Q* at a given point on the detector is given by

$$Q(r) = 4\pi(\sin\theta/2)/\lambda = 4\pi\left\{\sin\left[\left(\tan^{-1}\left(r/L_D\right)\right)/2\right]\right\}/\lambda \quad (1)$$

where *r* is the radial distance of a point on the detector from the beam axis, L_D the sample-to-detector distance, θ the scattering angle and λ the neutron wavelength. If we considered the closest distance at which reliable data may be recorded given by the smallest beam-stop and the largest distance given by

the detector corners, the *Q*-range available for a selection of instrument configuration is shown in figure 6.

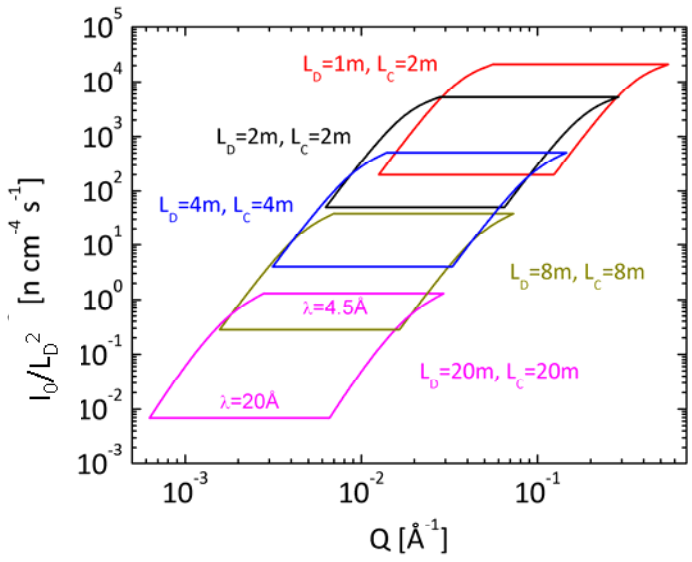

Figure 6. Available range of momentum transfer *Q* for a selection of instrument configurations at KWS-2: the neutron flux at the sample position divided by the square of the detector distance is plotted against *Q* for different combinations of collimation length L_C and detection length L_D and for neutron wavelengths in the range 4.5Å ≤ λ ≤ 20Å.

3.3 Beam Profile

A very important quantity in the characterization of the instrument is the contrast ration at the detector. This is defined by the peak intensity in the center of the beam stop versus the flux at twice the half-widths of the primary beam. As can be seen from the intensity distribution in figure 7, the contrast ratio is of the order of 10^5, which allows measurements of very small scattering cross-sections.

3.4. Instrument resolution

One of the elements enabling for the achievement of a high neutron flux on the sample is the large wavelength spread used, $\Delta\lambda/\lambda=0.20$. The large $\Delta\lambda/\lambda$ and the limited geometric resolution of a SANS instrument (finite collimation, detector resolution, gravity) lead to smearing that can cause to a certain extent loss of the structural information contained in the SANS curve. In order to recover at least part of this information lost as a result of the limited resolution, the actual instrumental resolution parameters have to be known a priori or determined independently. The structural information is then retrieved usually by implementing the resolution function in the fitting procedure [11] or, less used, by desmearing the measured data [12]. The resolution of pinhole SANS instruments with area detectors is well understood and can be modeled according to [11, 13, 14]. At KWS-2 the wavelength distribution measured by time-of-flight [6] agrees well with that resulting from the setting of the mechanical velocity selector, a Gaussian-like distribution with $\Delta\lambda/\lambda=0.20$. For long wavelengths ($\lambda>10$Å), the wavelength distribution deviates slightly from the triangular form and becomes gradually asymmetric as a consequence of combined effects arising from the Maxwell speed distribution of the incoming "white" neutron beam and the deterioration of the transmission and resolution of the velocity selector for large beam divergence characteristic for long neutron wavelengths [15].

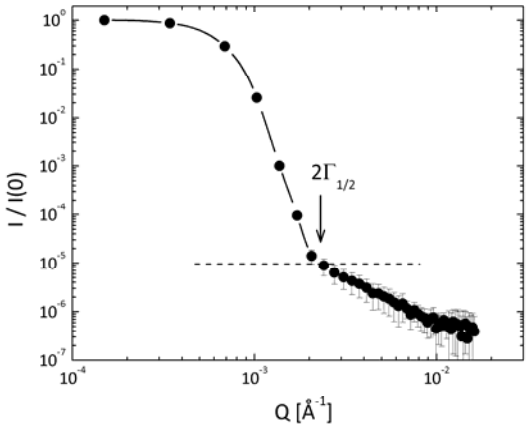

Figure 7. Intensity profile measured at KWS-2 for the collimation length L_C=8m, detection distance L_D=8m and λ=12Å.

A dilute dispersion of charged-stabilized, monodisperse silica nanoparticles has been used to verify the instrumental resolution function based on the wavelength spread provided by the velocity selector, the beam divergence determined by the collimation system and the cell size of the detector. The data measured with λ=4.5Å, corrected for detector sensitivity, instrument background, scattering from empty cell and solvent and calibrated on the absolute scale are displayed in figure 8 over the typical *Q*-range explored at KWS-2 by using different L_C-L_D combinations.

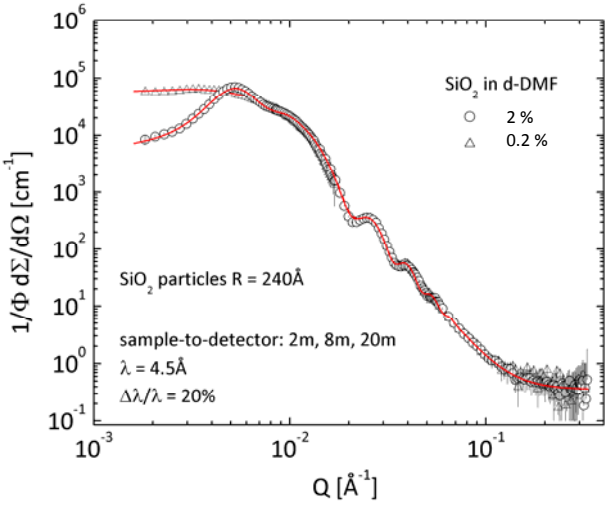

Figure 8. SANS patterns from silica particles in deuterated DMF for different particle volume fractions described by model function convoluted with the instrument resolution.

The experimental data were fitted by a model function characteristic for a system of hard spheres [16] convoluted with the resolution function of the instrument. The fit of the data was successful and the structure parameters of the reference samples determined from a SAXS experiment [17] were recovered. One should remark that, even with a significant higher wavelength spread such as

$\Delta\lambda/\lambda$=0.20, the structural features of the form factor can be observed up to the third oscillation, which enables a quite reliable interpretation of the measured data in terms of structural models.

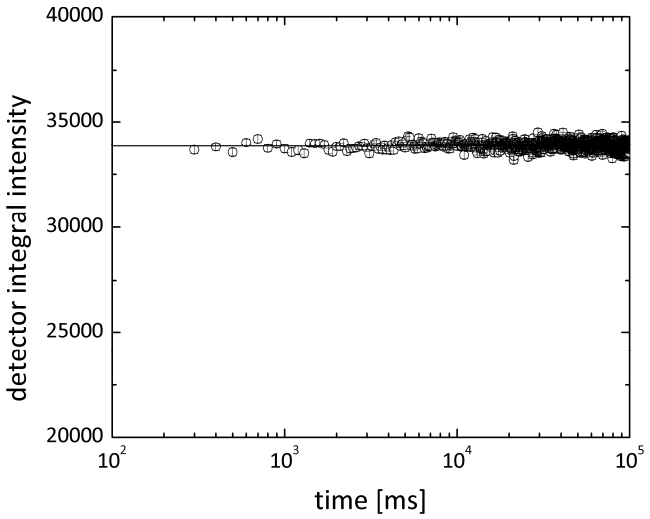

Figure 9. Fast SANS measurements of Plexiglas standard sample (isotropic constant pattern) performed with a time-resolution of 100ms as a test of the real-time data acquisition mode; final upgrade of the detection electronics allows for the fast start of data acquisition within 100ms after the opening of the instrument shutter.

3.5. Time-resolved SANS with 100ms time-resolution

KWS-2 was optimized for real time measurements of fast structural changes due to rapid kinetics. Data acquisition on sub-second time scale allows for the exploration of the early stages of formation of structures. Valuable new information are obtained in various soft matter topics like, for example, micellization behavior of block copolymers [18], fast crystallization of polymeric systems [19], deformation of elastomers [20] or application of magnetic fields [21]. At KWS-2, the detector electronics correlated with the experimental conditions (neutron wavelength and flight-path) allows for time-resolutions of the order of 100ms (figure 9). An example of time-resolved SANS study of the chain exchange kinetics in block copolymer micelles of spherical and cylindrical geometry is presented in [22].

4. Calibration and measurement methods

4.1. Wavelength calibration

The wavelength calibration is carried out by using Bragg reflection from silver behenate (AgBE powder supplied by Chemos GmbH, Germany), which is one of the very few materials that feature cold neutron Bragg reflections in the SANS angular range. These reflections (figure 10) can be analysed with Bragg's law to determine the wavelength of the primary beam delivered by the velocity selector [23,24], knowing the long-period spacing d=58.380Å of AgBE. The large particle size of the AgBE powder yields the scattering observed at low Q. The three Bragg peaks at high Q observed using different L_D's and various velocity selector speeds were analysed and the absolute wavelengths were determined.

4.2. Absolute intensity calibration

One of the advantages of the SANS technique is that the scattered intensity can be obtained on the absolute scale [25] and thus quantitative information such as molecular weight of polymers or aggregation number of micelles can be directly extracted from the "forward scattering" I($Q \rightarrow 0$). The absolute calibration of the scattering from a sample of interest is performed by scaling the recorded intensity with that from a sample (standard) with well known scattering properties. One of the typical standard samples used in neutron scattering is vanadium. Because of the weak scattering of vanadium, vanadium-calibrated materials are typically used as secondary standards for SANS. The secondary standard sample used at KWS-2 is a Plexiglas slab with a thickness of 1.5mm.

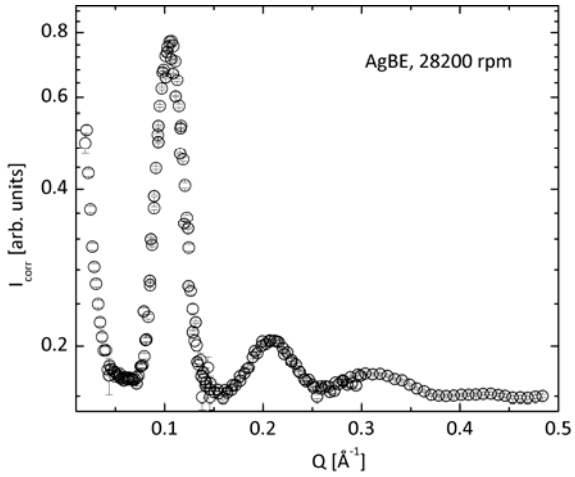

Figure 10. Scattering pattern from AgBE measured for the selector speed of 28200 rpm at three detection distances and corrected for detector sensitivity and background (instrument and cell).

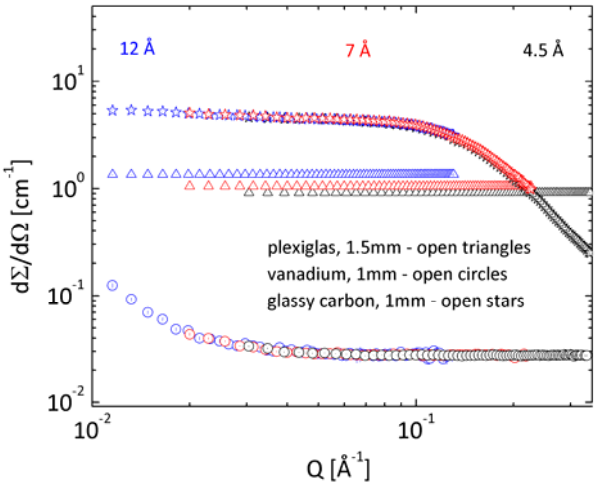

Figure 11. Absolute scattering cross-section from KWS-2 Plexiglas secondary standard for three different wavelengths: the data were calibrated with vanadium and cross-checked with glassy carbon.

The Plexiglas standard is calibrated with vanadium and, in order to account for multiple scattering effects, a cross-check with a glassy carbon standard sample [26] was done. This complex calibration procedure applied to the Plexiglas secondary standard allowed for a precise determination of the wavelength dependent calibration factor [24], which is further used for the absolute calibration of the scattering from the studied samples.

At KWS-2 the Plexiglas secondary standard is used also to normalize the individual detection cells of the main detector for local variations in efficiency (the detector sensitivity measurement).

4.3. Data reduction

The scattering intensities recorded at KWS-2 from studied samples are corrected, calibrated and, in the case of isotropic scattering, radial averaged using standard procedure [25] by means of the QtiKWS data analysis software [27].

5. Future upgrades

The boosting of the instrument performance towards higher intensities and wider *Q*-range by means of focusing elements – the MgF_2 aspherical lenses [3-5] and tilted velocity selector is aimed in the near future. For this purpose the neutron lenses are currently installed inside the last collimation segment towards the sample position, between 2m and 1m in front of the sample. The lenses have been tested and the experimental arrangements for the high resolution and high intensity modes were optimized [5]. A set of 26 lenses grouped in three packages that can be automatically brought in beam will be used either separately or in a combined way, to match the focusing conditions for different neutron wavelengths and collimation-detection conditions. In order to suppress the scattering on phonons and to increase the transmission by a factor of 2 the lenses will be cooled at 70K. For the high resolution mode the lenses will be used in combination with a high resolution position-sensitive scintillation detector and a double-disc chopper. The high resolution detector with space resolution of 0.5mm is installed in a fixed position at 17m after the sample. It is designed to be parked in a housing in top of the main detector evacuated tube (see figure 1) and to be brought automatically in beam when needed and the main detector is parked in the end position at 20m after the sample. The housing and positioning system of the high resolution detector are currently in construction.

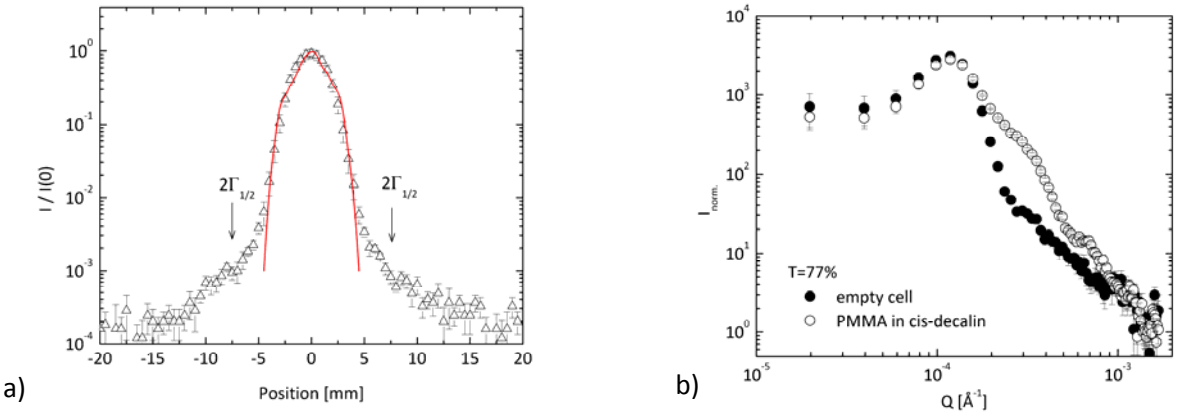

Figure 12. (a) – Focused beam profile obtained at KWS-2 using seven aspherical lenses as measured (symbols) and simulated (line) results; (b) – the scattered intensity from 0.25% PMMA in cis-decalin solution obtained by focusing-lenses at KWS-2; a beam-stop attached on the high resolution detector masks to a large extent the transmitted beam while the scattering from the sample is clearly observed above the background (empty cell) at $Q>2\text{x}10^{-4}$ Å^{-1}.

The high resolution mode combining the high resolution detector with aspherical MgF_2 lenses was tested at KWS-2. Figure 12a shows the beam profile measured while using seven lenses at room temperature and a neutron wavelength λ=18Å. The high resolution detector was placed at 8.9m distance from the lenses (7.1m after the sample) and the collimation length used was 20m (18.2m in front of the lenses) with an entrance aperture of 8x8 mm^2 and a sample aperture of 10x20 mm^2. The measured profile agrees very well in the central part with the results of simulations carried out using the McStas package with focusing lens compound [28] included. The contrast ratio obtained in these conditions is about 10^{-3} while the significant background observed towards the edge of the detector may arise from chromatic aberration (due to the large wavelength spread used) and scattering from the instrument windows. Definitely, these imperfections remain to be further improved.

Figure 12b shows in the radial averaged presentation the scattering from a sample of PMMA colloids in cis-decalin solution (1mm thickness) compared with the scattering from the empty sample cell. The signal from the sample is clearly visible above the background at $Q>2x10^{-4}Å^{-1}$. Corrected data are shown in figure 13 in parallel with the results obtained at KWS-2 with λ=7Å using the pinhole mode and at KWS-3 mirror-focusing instrument [29] with λ=12.7Å. The minimum Q value reached at KWS-2 with neutron lenses goes down to $10^{-4}Å^{-1}$, which shows that in the near future more than three decades in Q range, from $0.5Å^{-1}$ up to $10^{-4}Å^{-1}$, can be covered at a single instrument. A fit with the solid sphere form factor including the polydispersity $\sigma(R)/R$ of the particle radii reported by static light scattering (σ_0=0.06 of the log-normal size distribution), which is depicted by the solid curve in figure 13, delivered a colloidal radius of about 8100Å,, a value similar to that of 7900Å obtained by static light scattering. Because of finite resolution, the minima of the form factor are smeared out in the experimental data measured using both focusing methods.

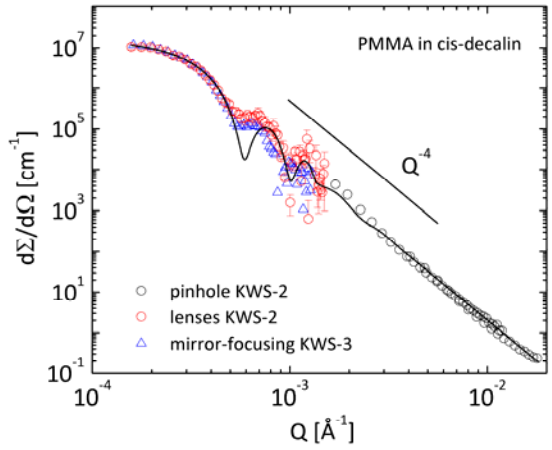

Figure 13. Intensity versus scattering vector of the 0.25% PMMA in cis-decalin solution obtained at KWS-2 by combining the classical pinhole and lenses-focusing modes. The data measured on the same sample at KWS-3 mirror-focusing instrument are shown in parallel. The solid curve represents the fit of the experimental data with the form factor of spheres (see text).

In order to have thus the possibility to tune the wavelength resolution for the conventional pinhole mode and to avoid the chromatic aberration effects while using the focusing lenses the analysis of the wavelength distribution by time-of-flight using a double-disc chopper with variable opening is planned to be used. The installation of the chopper in front of the collimation is currently in progress. The two discs with two diametrically opposed windows (90° sectors) are placed very close to each other (5cm). Thus, a variable opening of the chopper can be achieved by changing the phase between the discs

which will allow for a high flexibility with respect to defining the time resolution and intensity on the sample.

Finally, the possibility to explore larger Q domains, up to 1Å^{-1}, is targeted in close connection to the small correlation lengths typically exhibited by biological structures.

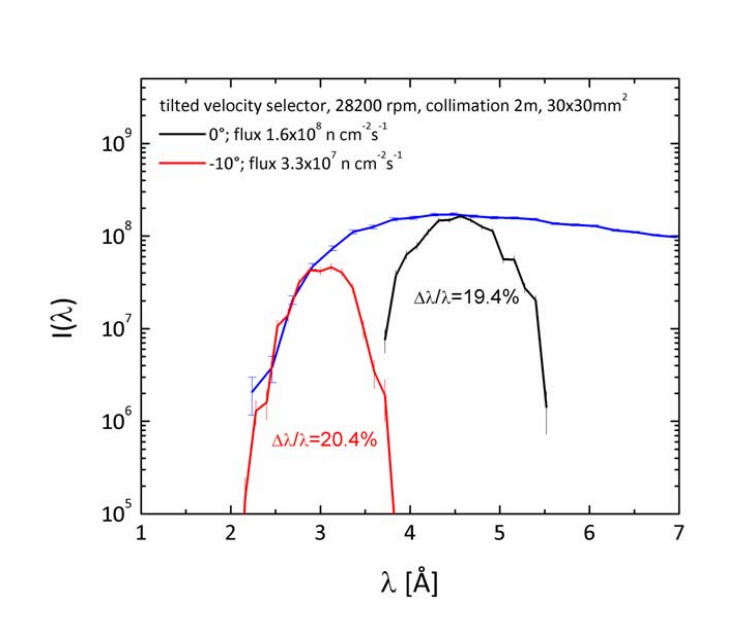

Figure 14. Simulated results at the end of the vertical "S-shaped" NL3a-o guide obtained for the white flux (blue line) and the monochromatic flux (black and red lines) using the velocity selector at a speed of 28200 rpm in two tilting situations (0° and -10° with respect to the beam axis).

For this purpose a vertical tilting of the velocity selector up to -10° with respect to the beam axis is intended. One should mention that the velocity selector is placed in the middle of the vertical "S-shaped" guide with the entrance window in a "*three o'clock*" position. Simulations carried out with McStas package [30] have shown that the neutron wavelength of λ=3Å ($Q_{max} \rightarrow 1\text{Å}^{-1}$) can be selected with certain advantages prevailing over the disadvantages: due to the cut-off of the "S-shaped" neutron guide the wavelength spread (20%) is held while the price in intensity is acceptable for the low resolution–high intensity (shortest sample-to-detector distance) configuration aimed in this situation. The mechanism for the controlled vertical tilting of the selector is in construction phase and will be installed in the summer of 2012.

6. Conclusions

KWS-2 instrument operated by the JCNS at FRM II is a high intensity / wide Q-range small-angle neutron diffractometer optimized for studies of soft-matter and biological systems. The high intensity permits on one hand rapid measurement of small or weak-scattering samples and, on the other hand, time-resolved structural investigations with a time resolution up to 100ms. The possibility to cover up to four decades in Q, between $1\text{x}10^{-4}\text{Å}^{-1}$ and 1Å^{-1}, will enable structural studies over a wide length scale spanning between several Å and 1μm.

Acknowledgements

The constant help for operating, optimizing and upgrading the KWS-2 instrument from M.Heiderich, R.Hanslik, S.Staringer, H.Schneider, T.Kohnke, U.Bünten, R.Engels, G.Kemmerling, M.Wagener, M.Drochner, L.Fuss-Fleischhauer, R.Möller, F.Suxdorf and H.Kleines (all Forschungszentrum Jülich

GmbH) is gratefully acknowledged. We thank J.Stellbrink (Forschungszentrum Jülich GmbH) for the kindness to provide us the KWS-3 and pinhole KWS-2 SANS data on PMMA. Kind supply of the glassy carbon standard sample characterized with SAXS by J.Ilavsky (Argonne National Laboratory) and of SiO_2 size-standard sample by W.Sager (Forschungszentrum Jülich GmbH) is acknowledged. We thank D.Schwahn (Forschungszentrum Jülich GmbH) for useful discussions and his valuable advices with respect to the operation and development of KWS-2.

References

[1] Gläser W and Petry W 2000 *Physica B* **276-278** 30
[2] Radulescu A and Ioffe A 2008 *Nucl. Instr. and Meth. A* **586** 55
[3] Choi S M, Barker J G, Glinka C J, Cheng Y T and Gammel P L 2000 *J. Appl. Cryst.* **33** 793
[4] Koizumi S, Iwase H, Suzuki J, Oku T, Motokawa R, Sasao H, Tanaka H, Yamaguchi D, Shimizu H M and Hashimoto T 2007 *J. Appl. Cryst.* **40** s474
[5] Frielinghaus H, Pipich V, Radulescu A, Heiderich M, Hanslik R, Dahlhoff K, Iwase H, Koizumi S and Schwahn D 2009 *J. Appl. Cryst.* **42** 681
[6] Radulescu A, Pipich V and Ioffe A. *Nucl.Instr. and Meth. A* submitted
[7] Heiderich M, Reinartz R, Kurz R and Schelten J 1991 *Nucl. Instr. And Meth. A* **305** 423
[8] Engels R, Clemens U, Kemmerling G, Nöldgen H and Schelten S 2009 *Nucl. Instr. And Meth. A* **604** 147
[9] Kemmerling G, Bünten U, Clemens U, Engels R, Heiderich M, Pyckhout-Hintzen W, Rongen H, Schelten J, Schwahn D and Zwoll K 2004 *IEE Trans. Nucl. Sci.* **51** 1098
[10] Zeitelhack K et al. 2006 *Nucl. Instr. and Meth. A* **560** 444
[11] Pedersen J S, Posselt D and Mortensen K 1990 *J.Appl.Cryst.* **23** 321
[12] Kline S R 2006 *J.Appl.Cryst.* **39** 895
[13] Pedersen J S 1997 *Adv. Colloid Interface Sci.* **70** 171
[14] Barker J G and Pedersen J S 1995 *J. Appl. Cryst.* **28** 105
[15] Friedrich H, Wagner V and Wille P 1989 *Physica B* **156-157** 547
[16] Mortensen K 1993 *Prog. Colloid Pol. Sci.* **93** 72
[17] Vad T, Sager W F C, Zhang J, Buitenhuis J and Radulescu A 2010 *J. Appl. Cryst.* **43** 686
[18] Willner L, Poppe A, Allgaier J, Monkenbusch M and Richter D 2001 *Europhys. Lett.* **55** 667
[19] Wang H 2006 *Polymer* **47** 4897
[20] Burford R P, Markotsis M G and Knott R B 2006 *Physica B* **385-386** 766
[21] Wiedenmann A, Keiderling U, Meissner M, Wallacher D, Gähler R, May R P, Prevost S, Klokkenburg M, Erne B H and Kolbrecher J 2008 *Phys. Rev. B* **77** 184417
[22] Lund R, Willner L, Pipich V, Grillo I, Lindner P, Colmenero J and Richter D 2011 *Macromolecules* **44** 6145
[23] Keiderling U, Gilles R and Wiedenmann A 1999 *J. Appl. Cryst.* **32** 456
[24] Okabe S, Karino T, Nagao M, Watanabe S and Shibayama M 2007 *Nucl. Instr. and Meth.* **572** 853
[25] Lindner P 2002 Neutrons, X-Rays and Light: Scattering Methods Applied to Soft-Condensed Matter, ed. Lindner P and Zemb Th (Elsevier – North Holland Delta Series, Amsterdam)
[26] Zhang F, Ilavsky J, Long G, Quintana J, Allen A and Jemian P 2010 *Metall. Mater. Trans.* **41** 1151
[27] http://iffwww.iff.kfa-juelich.de/~pipich/dokuwiki/doku.php/qtikws
[28] http://www.mcstas.org/download/components/contrib/Lens.html
[29] Kentzinger E, Dohmen L, Alefeld B, Rücker U, Stellbrink J, Ioffe A, Richter D and Brückel T 2004 *Physica B* **350** e779
[30] Willendrup P, Farhi E and Lefmann K 2004 *Physica B* **350** 735

Erratum

Figure 5 in the original paper incorrectly showed the absolute neutron flux for a CNS filling of 13l, which results in an increased flux at the sample position with a factor of up to 1.7. The correct figure and caption are shown below.

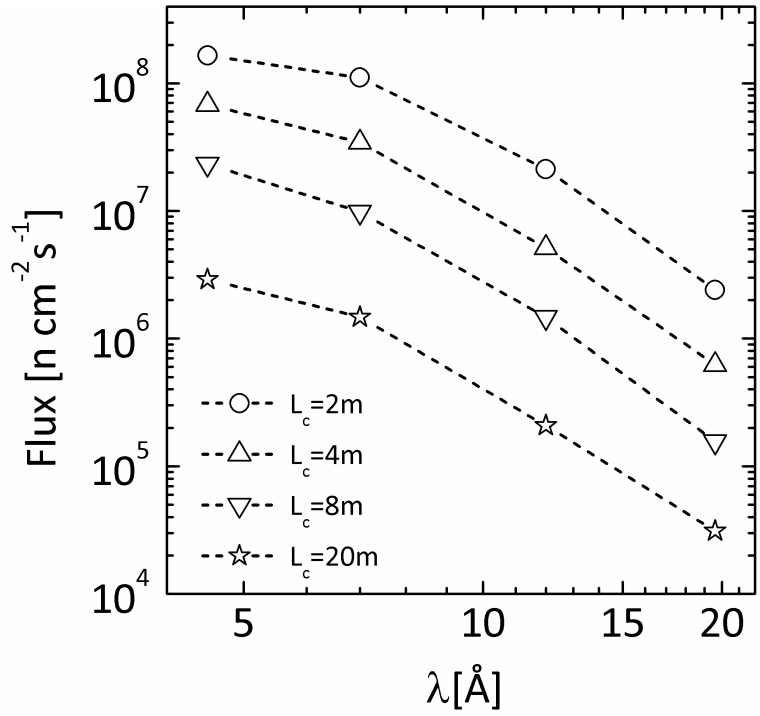

Figure 5. Absolute neutron flux at the sample position as a function of wavelength λ for different collimation lengths L_C, typical opening of the entrance and sample apertures and 10.6l CNS filling.